Computers in Biology and Medicine 163 (2023) 107085

Contents lists available at ScienceDirect

Computers in Biology and Medicine

journal homepage: www.elsevier.com/locate/compbiomed

Shared gene expression signatures between visceral adipose and skeletal muscle tissues are associated with cardiometabolic traits in children with obesity

Mireia Bustos-Aibar [a,1], Concepción M. Aguilera [a,b,1], Jesús Alcalá-Fdez [c,*], Francisco J. Ruiz-Ojeda [a,d], Julio Plaza-Díaz [a,e], Abel Plaza-Florido [f,g], Inés Tofe [b,h], Mercedes Gil-Campos [b,h], María J. Gacto [i], Augusto Anguita-Ruiz [a,j]

[a] Department of Biochemistry and Molecular Biology II, School of Pharmacy, University of Granada, 18071, Granada, Spain
[b] Biomedical Research Networking Center for Physiopathology of Obesity and Nutrition, Carlos III Health Institute, 28029, Madrid, Spain
[c] Department of Computer Science and Artificial Intelligence, Andalusian Research Institute in Data Science and Computational Intelligence (DaSCI), University of Granada, 18071, Granada, Spain
[d] RG Adipocytes and Metabolism, Institute for Diabetes and Obesity, Helmholtz Diabetes Center at the Helmholtz Zentrum München, Neuherberg, 85764, Munich, Germany
[e] Children's Hospital of Eastern Ontario Research Institute, Ottawa, ON K1H 8L1, Ontario, Canada
[f] PROmoting FITness and Health through physical activity research group, Sport and Health University Research Institute, Department of Physical Education and Sports, University of Granada, 18071, Granada, Spain
[g] Pediatric Exercise and Genomics Research Center, Department of Pediatrics, School of Medicine, University of California at Irvine, Irvine, 92617, CA, United States
[h] University Clinical Hospital, Institute Maimónides of Biomedicine Investigation of Córdoba, University of Córdoba, 14004, Córdoba, Spain
[i] Department of Software Engineering, University of Granada, 18071, Granada, Spain
[j] Barcelona Institute for Global Health, ISGlobal, 08003, Barcelona, Spain

ARTICLE INFO

Dataset link: https://github.com/COBLabUGR/WGCNAInterTis sueObesity

Keywords:
Childhood obesity
Gene co-expression
Hierarchical clustering
Inter-tissue molecular signatures
Skeletal muscle tissue
Visceral adipose tissue

ABSTRACT

Obesity in children is related to the development of cardiometabolic complications later in life, where molecular changes of visceral adipose tissue (VAT) and skeletal muscle tissue (SMT) have been proven to be fundamental. The aim of this study is to unveil the gene expression architecture of both tissues in a cohort of Spanish boys with obesity, using a clustering method known as weighted gene co-expression network analysis. For this purpose, we have followed a multi-objective analytic pipeline consisting of three main approaches; identification of gene co-expression clusters associated with childhood obesity, individually in VAT and SMT (intra-tissue, approach I); identification of gene co-expression clusters associated with obesity-metabolic alterations, individually in VAT and SMT (intra-tissue, approach II); and identification of gene co-expression clusters associated with obesity-metabolic alterations simultaneously in VAT and SMT (inter-tissue, approach III). In both tissues, we identified independent and inter-tissue gene co-expression signatures associated with obesity and cardiovascular risk, some of which exceeded multiple-test correction filters. In these signatures, we could identify some central hub genes (e.g., *NDUFB8, GUCY1B1, KCNMA1, NPR2, PPP3CC*) participating in relevant metabolic pathways exceeding multiple-testing correction filters. We identified the central hub genes *PIK3R2, PPP3C* and *PTPN5* associated with MAPK signaling and insulin resistance terms. This is the first time that these genes have been associated with childhood obesity in both tissues. Therefore, they could be potential novel molecular targets for drugs and health interventions, opening new lines of research on the personalized care in this pathology. This work generates interesting hypotheses about the transcriptomics alterations underlying metabolic health alterations in obesity in the pediatric population.

* Corresponding author.
E-mail addresses: bustosaibar@gmail.com (M. Bustos-Aibar), caguiler@ugr.es (C.M. Aguilera), jalcala@decsai.ugr.es (J. Alcalá-Fdez), fjrojeda@ugr.es (F.J. Ruiz-Ojeda), jrplaza@ugr.es (J. Plaza-Díaz), abeladrianplazaflorido@gmail.com (A. Plaza-Florido), drakaramelo@hotmail.com (I. Tofe), mercedes_gil_campos@yahoo.es (M. Gil-Campos), mjgacto@ugr.es (M.J. Gacto), augusto.anguita@isglobal.org (A. Anguita-Ruiz).
[1] These authors contributed equally to this work.

https://doi.org/10.1016/j.compbiomed.2023.107085
Received 25 November 2022; Received in revised form 28 April 2023; Accepted 27 May 2023
Available online 14 June 2023

1. Introduction

Childhood obesity is one of the leading health concerns of recent decades [1]. Low-grade systemic inflammation along with insulin resistance are key components in the metabolic alterations associated with childhood obesity, which unleash the emergence of cardiovascular disease (CVD), as well as type 2 diabetes (T2D) in adulthood [2–4]. Low-grade systemic inflammation is mainly due to the infiltration of immune cells into the adipose tissue producing the dysregulation of its endocrine function [5]. Adipose tissue is mainly distributed throughout the body as subcutaneous and visceral adipose tissue (VAT). Metabolic disorders are more strongly linked to alterations in VAT compared with subcutaneous depots, highlighting the association with hypertension, diabetes, insulin resistance, increased mortality, hepatic steatosis, and atherosclerosis, among others [6].

Importantly, not only adipose tissue is implicated in developing obesity metabolic alterations. Dysregulation of skeletal muscle tissue (SMT) metabolism can also influence developing insulin resistance and alter whole-body glucose homeostasis [7]. VAT and SMT interact with each other through the secretion of proteins with a key role in controlling metabolic health (adipokines and myokines, respectively); and this is known as the VAT-SMT metabolic axis [8,9]. The molecular mechanisms involved in obesity-associated inflammation and altered metabolism in VAT and SMT were assessed separately [10,11]. Interestingly, some pathways, such as *IL-6* and *IL1B* have been extensively described as simultaneously dysregulated in both tissues in middle-aged adults with severe obesity, leading to the appearance of metabolic dysfunction [12]. However, to the best of our knowledge, the concerted biological mechanisms and gene expression signatures affecting the inter-tissue metabolic homeostasis associated with obesity in children are not yet known.

In biological systems, genes are organized into networks following a free-scale network topology (i.e., a network with a few highly interconnected central genes and many poorly connected peripheral genes) [13]. Understanding the structure of human gene expression networks and their dysregulation is essential to identify relevant molecular targets implicated in the physiopathology of multifactorial diseases, such as obesity. With the aim of discovering patterns and relationships that underlie human gene expression networks, Artificial Intelligence techniques, and especially those of Machine Learning (ML), have been successfully applied [14]. Clustering is one of the ML techniques most widely used in bioinformatics. This technique identifies natural groups in data, allowing scientists to better interpret and understand biological processes that govern systems at the molecular level [15–17]. A wide range of clustering methods have been developed to address common research challenges in transcriptomics, such as the identification of epistasis phenomena [18] and the integration of inter-tissue gene expression signatures [19]. Among them, a hierarchical clustering technique for the identification of gene–gene relationships named Weighted Gene Co-expression Network Analysis (WGCNA) is of particular interest [20,21]. WGCNA is defined as a clustering method that, based on similarity, correlation and distance measures, identifies gene groups with similar expression patterns in a set of samples. Thus, by transforming unprocessed expression values in organized, interconnected and clustered charts; it can uncover concealed patterns in the initial dataset. The application of WGCNA to transcriptomic data from two different tissues (VAT and SMT) would allow the discovery of concerted gene co-expression patterns altered in different tissues and linked to a specific disorder, such as obesity.

In this study, we applied WGCNA to the entire genome-wide association data from SMT and VAT with the aim of revealing co-expression clusters, as well as their ontological functions associated with obesity and metabolic dysfunction in children. The specific aims of this study are: (I) Identification of the gene co-expression clusters associated with childhood obesity, individually in VAT and SMT (intra-tissue approach), (II) Identification of the gene co-expression clusters associated with obesity-metabolic alterations, individually in VAT and SMT (intra-tissue approach), and (III) Identification of the gene co-expression clusters associated with obesity-metabolic alterations simultaneously in VAT and SMT (inter-tissue approach). Moreover, we have developed a web page associated with this paper (i.e., https://sci2s.ugr.es/WGCNAInterTissueObesitys) with supplementary material for this study.

2. Materials and methods

2.1. Experimental design and study population

The study population was composed of 12 Spanish children (11 boys, 1 girl), aged 6–12. Participants were diagnosed with a false-positive prognosis of severe appendicitis or a hernia and underwent abdominal surgery at the Pediatric Surgery Department of the Reina Sofía Hospital, University of Cordoba, Spain. The criteria of Cole et al. (2000) were used to determine the obesity status [22]. 11 participants had an adequate VAT sample (6 normal-weight [5 boys] and 5 boys with obesity [all boys]), whereas the number of children with suitable SMT sample was 10 (5 normal weight [4 boys] and 5 boys with obesity [all boys]). The 5 boys with obesity and 3 boys and 1 girl with normal-weight coincided in both sample groups (VAT and SMT), presenting valid samples for both tissues. A summary of the study design can be found in Fig. 1.

Tanner's criteria was utilized to define the pubertal stage [23] and corroborated by blood sex hormone levels. The inclusion criteria for the study population were: pre-pubertal state; age from 5 to 14 years old; and non-existence of syndromic obesity. Exclusion criteria were: pubertal state (Tanner II-V); the presence of malnutrition or illness; along with the use of medications that alter glucose or lipid metabolism and blood circulation. Supplementary details regarding the study design can be found elsewhere [24].

2.2. Biochemical and anthropometric determination

Body weight (kg) and height (cm) were measured using standardized procedures, and body mass index (BMI) was determined. BMI Z-Score was then estimated following the reference table of Sobradillo et al. [25]. Systolic blood pressure (SBP) and diastolic blood pressure (DBP) were assessed by the same trained professional according to international guidelines [26]. Fasting blood samples were obtained before surgery using venipuncture and stored at −80 °C until further analysis. Glucose levels were quantified using the glucose oxidase method; and plasma insulin concentrations were analyzed via radioimmunoassay [24]. The insulin resistance index was computed as the homeostatic assessment model for insulin resistance (HOMA-IR) [27]. The quantitative insulin sensitivity check index (QUICKI) was also calculated as described by Katz et al. (2000) [28]. Total leptin concentrations were determined by ELISA (BioSource International Inc., Camarillo, CA, USA). Plasma high density lipoprotein (HDL-c), low density lipoprotein (LDL-c) and total cholesterol, as well as apolipoprotein A1 (Apo-A) and B (Apo-B) levels, were obtained using an automatic analyzer (Roche-Hitachi Modular P and D Autoanalyzer). Importantly, when referring to any of the abovementioned variables we will use the term cardiometabolic traits.

2.3. Descriptive statistics and microarray analysis

The normality of all continuous variables was assessed. Shapiro–Wilk tests were performed and variables were transformed when necessary. Levene's test means was used to check for heteroscedasticity. Next, the Mann–Whitney U Test and t-test were then implemented in accordance with standard assumptions to identify group dissimilarities. We evaluated the effect of confounding variables such as age and sex by studying its differences between groups with a t-test, and its correlation

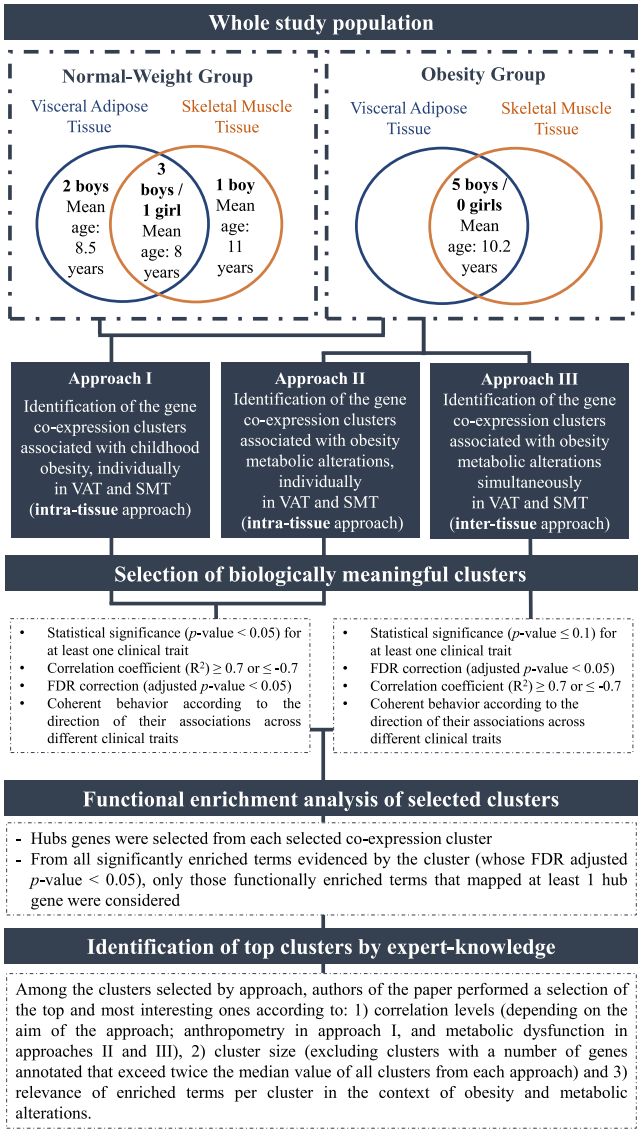

Fig. 1. Study population details and overall analysis plan. Further supplementary information concerning the objectives and specific goals of each approach can be referenced in Section 3 of the associated supplementary website linked to this manuscript.

with the first two principal components of the filtered gene dataset of each tissue. In any case, no significant associations were found. Furthermore, any children in our population showed signs of puberty entrance (evaluated by trained pediatricians using Tanner Scale) [23], which could be the main source of chronological variability in molecular profiles. It should be noted that the correlation of a cluster with age was also considered as exclusion criterion in the cluster selection ((R2 > |0.7| or *p*-value < 0.05)), please see Section 2.6 of this manuscript for further information.

2.4. Data pre-processing and feature selection

Fluorescence intensity cues per individual and tissue samples were obtained from microarray analyses. The quality of transcriptomic raw CEL files was evaluated with R (version 4.2.1) [29]. Since clustering algorithms based on similarity criteria are very sensitive to differences in the magnitude or scales of the data [30,31], a multi-chip robust mean normalization strategy was applied. All genes were annotated according to the current version of *org.Hs.eg.db* database [32]. Affymetrix microarrays provide an initial number of genes higher than 30,000. Data acquisition based on high-throughput technology often faces missing values attributable to insufficient resolution, fabrication errors, and poor hybridization, among others [33–35]. Missing data was removed since its presence may entangle the use of clustering algorithms and lead to spurious conclusions.

We were interested on the reduction of the dimensionality space of the whole genome to genes whose behavior is relevant for the disease that we were studying. On this reduced search space, we focus on generating co-expression networks that allowed the identification of molecular patterns or signatures in each tissue, to unveil which pathways or biological functions are altered individually and simultaneously, in the context of obesity and metabolic syndrome. The reduction of the whole genome dimensionality with feature selection based on expert knowledge is key to find relevant patterns and not to mislead in the immensity of genes that can sometimes lead to spurious associations [15,16]. Considering this, and focusing on the biological relevance and comprehensibility of the clustering algorithms with micro-array data [36], we performed a Differential Expression (DE) analysis to decrease the initial number of genes. Therefore, DE genes found in each tissue when comparing normal-weight subjects versus boys with obesity within each tissue group (nominal *p*-value < 0.05 and signal log-ratio > |1|, in any comparison) were selected. The effect of co-founding variables (i.e., age, height and sex) was evaluated correlating them with the first principal components of gene datasets. We did not included them in DE analysis since there were no significant differences found between normal-weight and obesity groups. The resulting normalized data set for each tissue group was formatted according to WGCNA R package requirements [37].

2.5. Knowledge-extraction phase: WGCNA approach

The WGCNA package supplies R functions for performing co-expression network analysis of genome-wide expression data. It uses hierarchical average linkage clustering to group genes with similar expression levels (e.g., all up-regulated or all down-regulated) [38–40]. The WGCNA procedure was implemented here following three different approaches (which are also summarized in Fig. 1):

Approach I. Intra-tissue WGCNA considering all participants. In this approach, gene expression data from VAT was analyzed in 11 children (5 with obesity and 6 normal-weight); as well as from SMT in 10 children (5 with obesity and 5 normal-weight). We aimed to identify the intra-tissue gene co-expression clusters associated with cardiovascular risk and the development of obesity in prepubertal children, individually in VAT and SMT.

Approach II. Intra-tissue WGCNA considering only boys with obesity. In this approach, only the VAT from 5 boys with obesity and the SMT from the same 5 boys with obesity were selected as valid gene expression data. We aimed to identify the intra-tissue gene co-expression clusters associated with obesity metabolic alterations and cardiovascular risk within each tissue in prepubertal boys with obesity, individually in VAT and SMT.

Approach III. Inter-tissue WGCNA considering only boys with obesity. This third approach aimed to identify the co-expression clusters from VAT and SMT correlated with altered metabolism and cardiovascular risk in obesity simultaneously in both tissues. Inter-tissue analyses were thus performed using VAT and SMT data from the same individuals.

It should be noted that in this study we have sequencing information from abdominal surgery performed on children so, given the logistical difficulties associated with obtaining such data, the sample size considered is inevitably small.

Section 3 of web associated with this paper describes in detail the steps followed for each of the above-mentioned approaches and

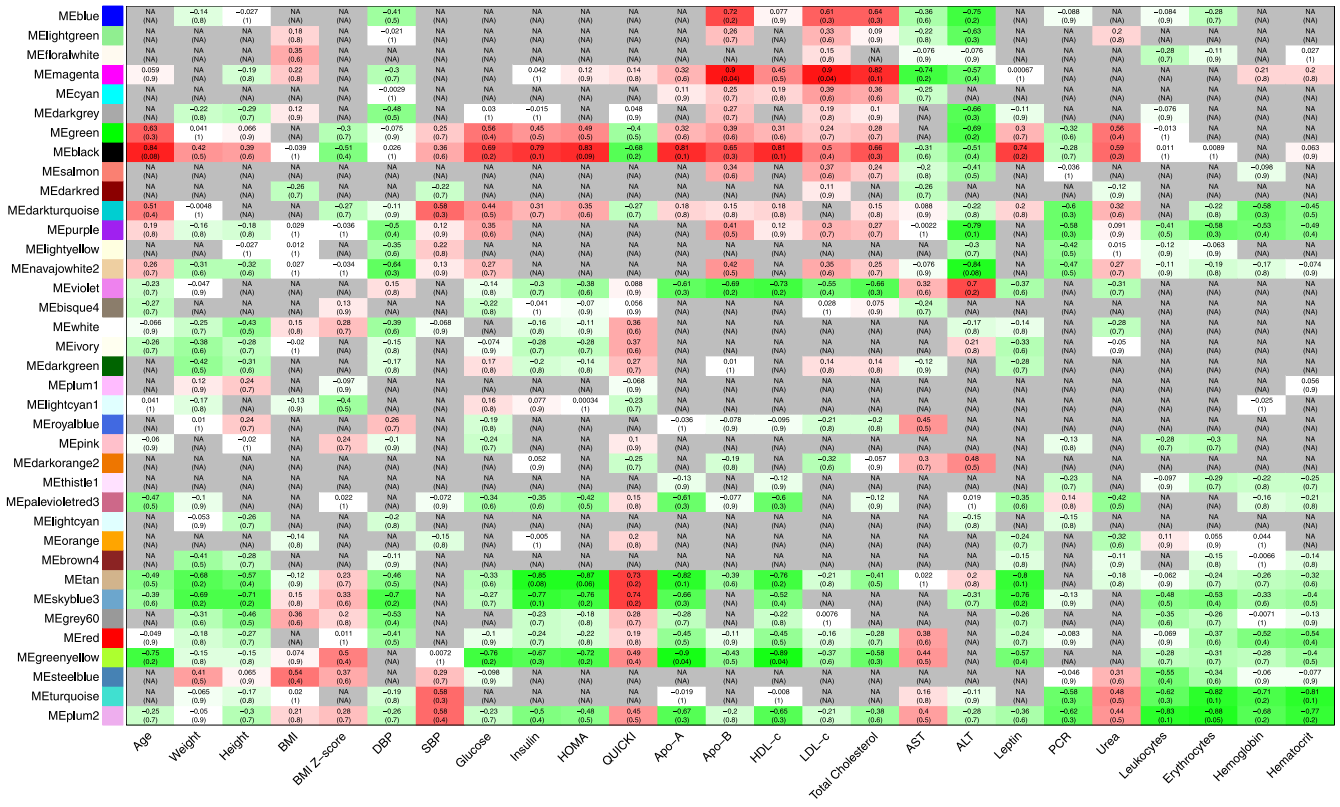

Fig. 2. Graphical characterization of associations among eigengene co-expression cluster vectors along with cardiometabolic traits from childhood obesity (Inter-tissue Approach III). Associations may be observed as correlation values (*p*-values). Each row corresponds to a co-expression cluster and each column to a trait. Each cell contains the corresponding correlation coefficient and nominal *p*-value. The table is color-coded by correlation according to the color legend. A higher resolution version of this figure is available on the website associated with the supplementary material of this paper, found in Section 4 (Fig. 20).

provides additional information regarding their purpose and interrelationships.

A deep description of the steps implemented for each of the above-mentioned approaches can be found in the paper's web Section 3. We strongly encourage readers to take a look of this section to get a better understanding of the findings that will be presented in next sections.

2.6. Functional validation of findings: criteria for considering clusters as biologically meaningful

To highlight the most relevant co-expression clusters (among all identified) in the framework of childhood obesity and its metabolic alterations, correlation coefficients between eigengene co-expression cluster vectors and cardiometabolic traits were evaluated. Their association enabled us to classify each cluster as a risk or protection cluster, in terms of obesity and metabolic dysfunction. The criteria for considering a cluster as biologically meaningful were defined using statistical significance (nominal p-value < 0.05 [in the case of approaches I and II], and p-value ≤ 0.1 [in the inter-tissue approach III] for at least one cardiometabolic trait); as well as correlation coefficient (R^2), which had to be ≥ 0.7 or ≤ -0.7 to be considered. Those correlated with confounding variables (such as age) were discarded. It should be noted that the consideration of a different level of significance in the inter-tissue is justified due to the fact that the number of clusters considered is much larger and some of their correlations are refer to VAT and SMT individually, please see the large number of clusters with missing values in Fig. 2 that represent the mismatch between the genes of both tissues in each cluster.

Gene co-expression clusters positively correlated with weight, BMI Z-Score, DBP, SBP, glucose, insulin, HOMA, apo-B, LDL-c and total cholesterol; and negatively correlated with QUICKI, apo-A and HDL-c were considered to be risk co-expression clusters. On the contrary, clusters that negatively correlated with weight, BMI Z-Score, DBP, SBP, glucose, insulin, HOMA, apo-B, LDL-c and total cholesterol; and positively correlated with QUICKI, apo-A and HDL-c were considered to be protection co-expression clusters [24]. Among all co-expression clusters that exceeded the aforementioned thresholds, those that did not show consistent behavior according to the direction of their associations in different cardiometabolic traits were excluded.

Co-expression clusters selected according to these criteria were subjected to functional enrichment analysis in order to identify their component genes and map biological pathways. For this purpose, only eigen-genes or hub genes whose FDR-adjusted p-value from their correlation with cardiometabolic traits was < 0.05 and whose cluster membership degree was > 0.8 were selected [41]. Cluster membership refers to the correlation of a particular gene expression profile with its cluster eigengene vector. For more details on the concept of degree of membership and the selection of the soft thresholding power using scale-free topology fitting, refer to Section 3 of the website associated with this paper.

The Gene ontology (GO) as well as the Kyoto encyclopedia of genes and genomes (KEGG) databases were employed to extract functional information for each list of hub genes per cluster [42,43]. Of all significantly enriched terms evidenced by clustering (whose FDR-adjusted p-value < 0.05), we considered only those functionally enriched terms that mapped at least 1 hub gene.

Among the clusters selected by approach, a selection of the top and most interesting was performed according to: (1) correlation levels (depending on the aim of the approach: anthropometry in approach I, and metabolic dysfunction in approaches II and III), (2) cluster size (excluding clusters with a number of genes annotated that exceed twice the median value of all clusters from each approach) and (3) relationship of enriched terms per cluster with obesity and metabolic alterations.

Table 1
Descriptive statistics generated from an analysis of variance of cardiometabolic traits in the entire study population (N = 12).

Variables	Normal-weight		With obesity		FDR-Adj *p*-val
	6 boys/1 girl		5 boys		
Age (years)	8.57	(1.72)	10.2	(1.3)	0.618
Weight (kg)	34.66	(15.79)	55.8	(6.57)	0.166
Height (cm)	136.19	(14.78)	141	(8.94)	0.888
BMI (kg/m^2)	16.89	[14.73, 25.74]	28.3	[26.08, 29.50]	0.07
BMI Z-score	−0.25	(1.24)	3.12	(1.07)	**0.035**
DBP (mm Hg)	61.33	(7.42)	71.2	(12.56)	0.63
SBP (mm Hg)	111.33	(7.84)	123	(15.80)	0.63
Glucose (mg/mL)	84.57	(12.45)	89.2	(7.98)	0.888
Insulin (mU/L)	1.42	[0.62, 2.06]	2.5	[0.84, 5.30]	0.813
HOMA index	0.29	[0.11, 0.44]	0.53	[0.17, 1.28]	0.888
QUICKI index	0.51	(0.06)	0.45	(0.08)	0.813
Apo-A (mg/dL)	114.29	(29.62)	144.5	(10.47)	0.595
Apo-B (mg/dL)	71.29	(22.33)	61	(21.32)	0.888
HDL-c (mg/dL)	55	(14.58)	69	(18.46)	0.762
LDL-c (mg/dL)	86	(24.36)	81.9	(33.58)	0.958
Cholesterol (mg/dL)	155.14	(35.14)	162.75	(44.54)	0.958
Triglycerides (mg/dL)	59	[38.00, 150.00]	62.5	[35.00, 77.00]	0.958
AST (U/L)	20	(3.37)	20.25	(3.86)	0.958
ALT (U/L)	14.57	(3.87)	22.75	(5.12)	0.166
PCR (mg/L)	44.3	[4.50, 380.40]	15.2	72.00]	0.958
Urea (mg/dL)	24.29	(4.07)	23.8	(7.26)	0.958
Proteins (g/dL)	7.04	(0.54)	7.45	(0.58)	0.813
Calcium (mg/dL)	10.45	(0.65)	10.47	(0.15)	0.967
Sodium (mmol/L)	136.14	(2.67)	135.2	(3.83)	0.933
Potassium (mmol/L)	4.37	(0.57)	4.24	(0.23)	0.933
Chlorine (mmol/L)	100.71	(2.98)	99.6	(3.36)	0.888
TSH (mU/L)	1.74	[0.32, 8.50]	1.01	[0.62, 3.41]	0.958
T4 (ng/dL)	1.4	(0.37)	1.28	(0.10)	0.888
FSH (mU/L)	0.3	[0.20, 1.70]	0.6	[0.20, 1.00]	0.951
Testosterone (pg/mL)	0.48	(0.17)	0.6	(0.21)	0.813
Cortisol (nmol/L)	26.08	(15.44)	18.98	(16.99)	0.888
Leukocytes (cell n°)	14160	(6105.34)	13200	(4988.99)	0.958
Erythrocytes (cell n°)	4.65	(0.48)	4.68	(0.42)	0.958
Hemoglobin (g/dL)	12.76	(0.86)	13.16	(0.86)	0.888
Hematocrit (\%)	37.71	(3.38)	39.04	(3.00)	0.888

3. Results

A summary of descriptive statistics comparing the participants' cardiometabolic traits from the entire study population (N = 12) can be found in Table 1. The descriptive statistics according to tissue-type group can be found as a supplementary file in Section 1 of the website created for this paper. Details of laboratory gene expression microarray analyses are also shown on this paper's website as supplementary methods, specifically in Section 2.

In this study, we performed a feature selection step that resulted 6000 DE genes from VAT and SAT, of which 224 genes met the inclusion criteria in both tissue groups. WGCNA was performed and a summary of the revealed gene co-expression cluster structures can be found in Fig. 1. From approach I, we identified 10 co-expression clusters in VAT, 4 satisfying our quality selection criteria; and 11 co-expression clusters in SMT, 6 satisfying quality selection criteria. By incorporating both normal-weight and boys with obesity into the analysis, approach I (intra-tissue) aimed to identify co-expression clusters that were associated with anthropometric measurements. Otherwise, approaches II (intra-tissue) and III (inter-tissue), which only included boys with obesity, allowed the identification of cluster structures associated with cardiometabolic phenotypes. The clusters identified in the inter-tissue approach III represent the shared molecular networks of tissues, which were correlated with metabolic and cardiovascular risk dysfunction. We identified 15 VAT co-expression clusters from approach II, 5 of which satisfied our quality selection criteria; and 17 co-expression clusters in SMT, 7 of which exceeded our quality selection criteria. From approach III (inter-tissue), we distinguished 37 co-expression clusters (Fig. 2), 4 of which satisfied our quality selection criteria. The complete list of hub genes identified for each cluster selected according to approach is available in Section 3 of the paper's website (specifically in Table 2 to 6). Supplementary material regarding cluster-trait correlation results is accessible in Section 4 of the paper's website, which presents an in-depth examination of cluster-trait relationships by approach and tissue in Supplementary Fig. 16 to 20 and Tables 10 to 14. Functional enrichment analysis was performed on the selected clusters by only selecting hub genes for each cluster. Functional enrichment results and its selected hub genes for all approaches can be found on Section 5 of the paper's associated website. Top clusters by approach were then identified by authors according to correlation levels, cluster size and relevance of enriched terms to obesity.

3.1. Top gene co-expression clusters associated with anthropometrics measurements (intra-tissue approach I)

A summary of the most relevant clusters and pathways identified in approach I can be found in Fig. 3(A). In VAT, the grey-60 cluster stands out due to its protection correlation with obesity and cardiometabolic alterations (i.e., higher expression values for the genes from the cluster are associated with lower weight and BMI z-score). Likewise, the dark-grey cluster also stands out because of its risk correlation (i.e., higher expression levels associate with higher values of BMI and BMI z-score). Hub genes from these co-expression clusters include important obesity targets such as (e.g., *LEP, NDUFA2, NDUFB8, NDUFB9, NDUFS3, RHOQ, RPS6, SHC1, ITGA1, CD47, GLS2*). Among these hubs, the *LEP, NDUFB8, NDUFS3, SHC1* and *RPS6* genes passed the multiple comparisons tests and further mapped to interesting KEGG terms: "D-Glutamine and D-glutamate metabolism", "insulin signaling pathway" and "non-alcoholic fatty liver disease (NAFLD)". In SMT, we can highlight the green-yellow and dark-green clusters as a result of their protection correlation with obesity. The black cluster was also selected from SMT based on its risk correlation. Hub genes from mentioned co-expression clusters (e.g., *LIMD1, BAHD1,*

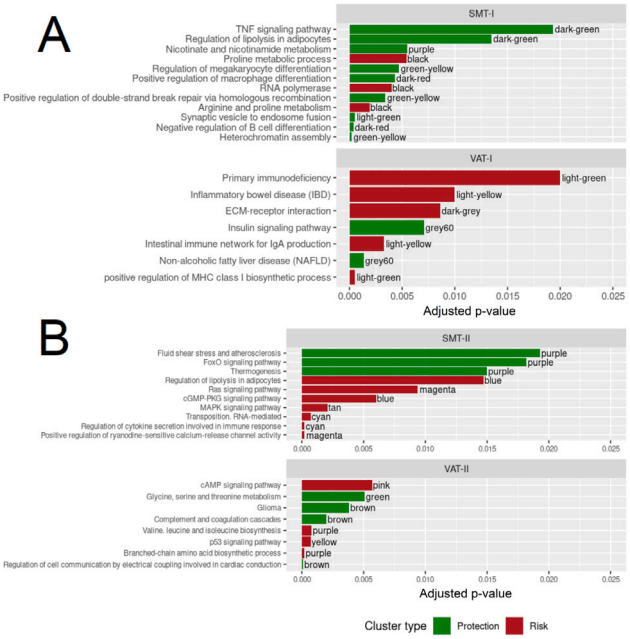

Fig. 3. Functional enrichment analysis for the top co-expression clusters identified in approaches I and II. (A) contains functional enrichment results for the top clusters in approach I, SMT and VAR respectively. (B) presents functional enrichment for the top clusters in approach II, SMT and VAT respectively. The *x*-axis gathers the enriched terms per cluster and the *y*-axis the significance of the enrichment (FDR-adjusted *p*-value < 0.05). The color of each cluster corresponds to its protection (green) or risk (red) correlation with obesity and cardiometabolic traits.

ACTR2, CNOT4, ASH2L, ABHD5, FABP4, RIPK1, CFLAR, MAP2K3, SERPINE1, ATF2, CCL5, ALDH4A1, POLR1C, POLR2J, POLR2J2, POLR2J3, PRKCA, VAMP4) mapped to significantly enriched functional terms such as "arginine and proline metabolism", "hippo signaling pathway - multiple species", as well as "TNF signaling pathway". Among these hubs, *PRKCA, SERPINE1* and *VAMP4* exceeded the FDR-Adjust *p*-value threshold. Given the nature of the experimental design of approach I (which included both normal-weight children and boys with obesity), the most significant correlations between grous and cardiometabolic traits identified were for anthropometric measures.

3.2. Top gene co-expression clusters associated with metabolic alterations (intra-tissue approach II)

A summary of the most relevant clusters and pathways identified in approach II can be found in Fig. 3 (C and D). In VAT, the green and brown clusters were highlighted due to their protection correlation with blood pressure (i.e., SBP, DBP), purple and pink by its risk correlation with lipid metabolism (i.e., LDL-c, apo-B and total cholesterol). Hub genes from these co-expression clusters (e.g., *GCSH, SARDH, IFNA7, ATG5, BCAT1, BCAT2, GCG, ADRB1, SST, PTGER3, CAMK2B, ATP1A3, ATP2B3, PDE4 A, ABCA1, APOE*) mapped to significantly enriched functional terms such as "branched-chain amino acid biosynthetic process", "cAMP signaling pathway", "cholesterol metabolism", "glycine, serine and threonine metabolism", and "RIG-I-like receptor signaling pathway". In SMT, the purple and grey-60 clusters stand out due to their protection correlation with lipid metabolism (i.e., HDL-c, LDL-c, apo-B and total cholesterol), while the magenta and cyan clusters for their risk correlation with glucose and lipid metabolism (i.e., glucose and LDL-c). Hub genes from these co-expression clusters (e.g., *ATP5F1E, DPF3, MAP2K3, MAPK14, PRKAA2, UQCR11, SMARCC1, TGFBR2, PRKAA2, TNFSF10, GABARAPL1, INHBB, E2F5, HACD2, FGFR1, FGFR2, PDGFRA, GNG4, CALM2, CALM3, CALM1, RASA4, RASA4B, ATG5*) mapped to significantly enriched functional terms per cluster: "fatty acid elongation", "foxO signaling pathway", "Ras signaling pathway", "regulation of cytokine secretion involved in immune response" "TGF-beta signaling pathway" and "thermogenesis".

3.3. Top gene co-expression clusters associated with metabolic alterations (inter-tissue approach III)

A summary of the most relevant clusters and pathways identified in approach III can be found in Fig. 4. As a reminder, this approach aimed to identify the shared molecular signatures associated with metabolic dysfunction simultaneously in both tissues (VAT and SMT) in boys with obesity. From this approach, we highlighted some clusters with a protection correlation with metabolic alterations (tan and skyblue-3, which correlated with HOMA and insulin), as well as some others with a risk correlation with metabolic dysfunction (magenta and green-yellow, which showed correlations with apo-B, LDL-c, apo-A and HDL-c). Hub genes from these co-expression clusters mapped to significantly enriched functional terms such as "adipocytokine signaling pathway", "cGMP biosynthetic process", "cGMP-mediated signaling", "insulin resistance", "lipid droplet formation", "MAPK signaling pathway", "NAFLD", "p53 signaling pathway", "positive regulation of SREBP signaling pathway", "valine. leucine and isoleucine biosynthesis" as well as "vascular smooth muscle contraction"; all of them strongly related to the molecular alterations of these tissues in the context of obesity. Some interesting hubs among these clusters that mapped those functional terms were *CALCRL, CD36, GUCY1B1, KCNMA1, MLX, NPR2, PPP3CC, PIK3R2, PTPN5, RXRA* and *SOCS3*. Among these hubs, *GUCY1B1, KCNMA1, NPR2* and *PPP3CC* exceeded the FDR-Adjust *p*-value threshold. Finally, we studied the convergence of results from both approaches since inter-tissue approach III jointly considered the fit to the free-scale topology criterion in each tissue. A Venn diagram for the hub genes identified in each of the intra-tissue approaches II (VAT and SMT) and III showed that the inter-tissue identified a large number of new hub genes that were not previously identified by the intra-tissue approach II, reinforcing the need to analyze this scenario (Fig. 5). Further information regarding the intersection between approaches and the hub-genes that were exclusively identified in consensus approach but not in approach II can be consulted in Section 3 of the paper's website (specifically in Tables 8 and 9).

4. Discussion

This study revealed the gene expression architecture of VAT and SMT in the context of obesity by using the clustering method WGCNA, following three different approaches. As a result, we identified both independent and inter-tissue gene expression clusters that were correlated with obesity and cardiovascular risk (Fig. 2). Functional enrichment analysis of the hub genes composing identified co-expression clusters from each approach revealed gene pathways that are strongly related to obesity and systemic metabolism. As far as we can appreciate, this is the first time the inter-tissue transcriptomic relationships have been assessed between VAT and SMT in the context of childhood obesity. As a result, we propose some interesting molecular mechanisms that might underlie muscle-adipose tissue cross-talk in obesity and metabolic dysfunction.

As might be expected from its study design, approach I individually identified co-expression clusters in VAT and SMT associated with anthropometric measurements. These co-expression clusters represent groups of genes whose expression is simultaneously up- or down-regulated in each tissue and whose overall expression profile is further correlated with the obesity degree in these children. In VAT, the genes that best characterized the identified clusters, known as hub genes, were involved in important biological pathways or disease routes by means of clusters such as "NAFLD", "insulin signaling pathway", and "ECM-receptor interaction", which are essential for the maintenance of metabolic homeostasis in obesity. This is interesting since there

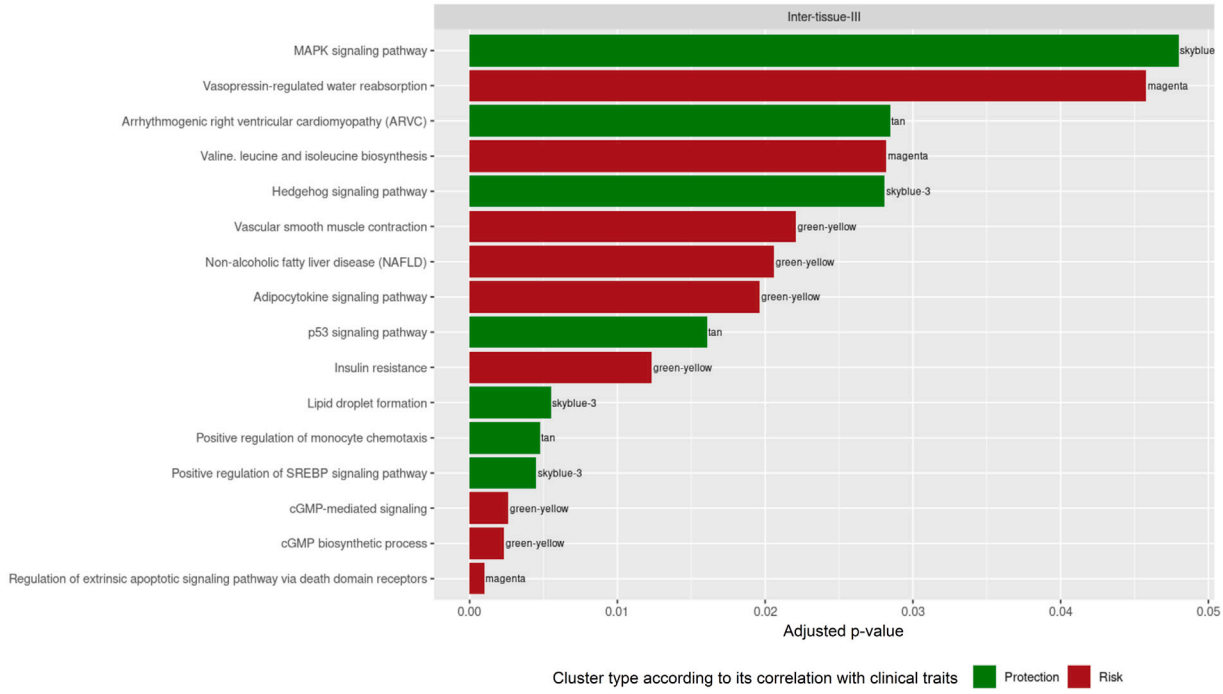

Fig. 4. Functional enrichment analysis for the top co-expression clusters identified in the inter-tissue approach III. The *x*-axis gathers the enriched terms per cluster and the *y*-axis the significance of the enrichment (FDR-Adjusted *p*-value < 0.05). The color of each cluster corresponds with its protection (green) or risk (red) correlation with obesity and cardiometabolic traits.

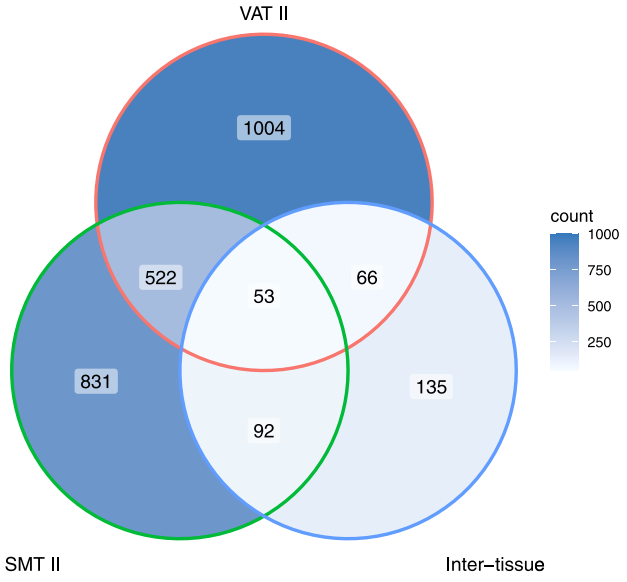

Fig. 5. Venn diagram of gene composition differences between hub genes from clusters from approach II and clusters from approach III (inter-tissue). There were 135 hub genes found in approach III that were not detected following the intra-tissue approach II, emphasizing the need for a joint analysis of both tissues.

is ample evidence showing that the expansion of unhealthy adipose tissue, mainly VAT, contributes to impaired insulin signaling, reduced ECM-receptor interaction due to accumulation of ECM components, and lipodystrophy with ectopic fat accumulation in the liver, which ultimately contributes to the development of NAFLD [44,45]. Among the most notable hub genes from the identified co-expression clusters, the hub genes from the grey-60 cluster stand out: the *LEP* gene, which maps the "NAFLD" biological term; and the *NDUF* family genes. *LEP* encodes leptin, a hormone secreted by the adipose tissue and one of the best-known key players in obesity [46,47]. The mitochondrial *NDUF* genes comprises key genes in the network, demonstrating their potential as biomarkers. Although the relationship of mitochondrial dysfunction and the development of obesity is known, this is the first time that the co-expression of several *NDUF* family genes in VAT in the setting of childhood obesity has been described. In SMT, otherwise, identified cluster hub genes were involved in biological pathways such as; "hippo signaling pathways", "TNF signaling pathway", "AGE-RAGE signaling" and "arginine and proline metabolism". It is worth mentioning that the hippo-signaling controls organ size, tissue homeostasis, nutrient-sensing pathways, and participates developing T2D, NAFLD along with cardiovascular disorders [47]. Interestingly, the hippo-signaling pathway also controls skeletal muscle growth and function [48]. Moreover, the "AGE-RAGE signaling" is an important pathway that controls the inflammatory cytokine secretion in SMT in obesity [49]. Mapping this term, we find the *TGFB1* hub gene (from the light-green module), which regulates growth, development and function of many metabolic tissues, including muscle. *TGFB1* is further implicated in energy homeostasis, and elevated TGF-β activity in ectopic adipocytes of SMT has been reported to induce cellular senescence, which may influence the metabolic status of muscle in obesity [50,51]. In summary, our approach I displays gene co-expression clusters associated with the presence of obesity and some metabolic traits in prepubertal children, individually in VAT and SMT. The detection of several hub genes, as well as enriched pathways previously associated with obesity, validate the relevance of our findings and yield new insights into the molecular networks underlying obesity in these tissues.

In Approach II, we identified gene co-expression clusters mainly associated with metabolic disturbances in boys with obesity, individually in the VAT and SMT. Specifically, in VAT, the expression profile of identified clusters was associated with lipid metabolism traits. In SMT, co-expression cluster profiles with a protective behavior were associated with lower values of the metabolic traits HDL-c, LDL-c, apo-B and total cholesterol. Their hub genes mapped the enriched terms; "thermogenesis", "FOXO signaling pathways", "TGF-β signaling pathway", and "fatty acid elongation". On the other hand, co-expression

clusters with risk correlation were associated with high levels of glucose metabolism traits and the terms; "Ras signaling pathway", "cGMP-PKG signaling pathway", "regulation of lipolysis in adipocytes", "regulation of cytokine secretion involved in immune response", and "MAPK signaling pathway". In general, from approach II, we found a strong concordance in terms of cardiometabolic traits correlated with each cluster expression profile and with their functional enrichment results for each cluster. For example, in the pink cluster (highlighted in VAT approach II), we found an association with lipid metabolism alterations (LDL-c, apo-B and cholesterol) while at the same time the functional enrichment analysis revealed how hub genes from this cluster map to biological pathways related to these phenotypes (e.g., "cAMP signaling pathway" and "cholesterol metabolism", highlighting the hub genes *APOE* and *ABCA1*). *APOE* and *ABCA1* are well-document molecular targets in the context of obesity [52,53]. The fact that both have been simultaneously detected as hubs in the same cluster indicates that they are perfect molecular targets, and that unknown targets of medical interest may be found in their cluster. In SMT approach II, the grey-60 and purple clusters were correlated with lipid metabolism, and further associated with functional terms such as "fatty acid elongation" and "thermogenesis". This concordance is fundamental for ensuring that the cardiometabolic trait correlations identified for each cluster are robust and reinforces the idea that such clusters are true representations of the molecular signatures correlated with obesity and metabolic risk. Lastly, from the inter-tissue approach III, we identified shared gene co-expression clusters between both tissues that were correlated with cardiometabolic traits in boys with obesity. Using this approach, we found both risk and protection clusters, showing associations with glucose and lipid metabolism traits (insulin, HOMA-IR, Apo-A, Apo-B, LDL-c and HDL-c). Hub genes from clusters with a protection profile mapped terms including; "lipid droplet formation", "MAPK signaling pathway", "p53 signaling pathway" and "positive regulation of SREBP signaling pathway". Among these terms, the MAPK signaling pathway (from the skyblue-3 cluster and including the hub genes *PPP3CC* and *PTPN5*), is one of the most interesting given its potential simultaneous role in both VAT and SMT. The MAPK route is implicated in the regulation of metabolism as a response to exercise in SMT, induces SMT inflammation [54], and acts as a pro-inflammatory factor in VAT [55]. Therefore, it is postulated as a perfect link between both metabolic tissues in obesity. The gene *PPP3CC* can modulate appetite and body mass and has also been linked to obesity [56]. The gene family *PTPN* is strongly linked with obesity, type 2 diabetes and adiposity [57,58]; however this is the first time that the gene *PTPN* has been linked with the metabolic pathology.

Taking this into account, we can state that the hub genes mapping this term (*PPP3CC, PTPN5*), as well as other hubs from the skyblue3 cluster, could be part of a complex polygenetic signature of metabolic alterations of obesity in both tissues. On the other hand, the co-expression clusters with risk correlation profile identified in this approach mapped the terms "valine, leucine and isoleucine biosynthesis", "insulin resistance", "adipocytokine signaling", "NAFLD", "vascular smooth muscle contraction", "cGMP biosynthetic process" and "cGMP-mediated signaling". Of these of particular interest is the term "insulin resistance" term, which points to a common metabolic disturbance found in both tissues, which indeed becomes systemic in the context of obesity. Mapping this term, we found that the *PIK3R2* (hub gene from the green-yellow cluster), and its expression in the VAT of T2D patients is higher compared to glucose tolerant subjects. Moreover, *PIK3R2* regulates phosphoinositide 3-kinase activity, an important enzyme in the insulin signaling pathway in both adipose and muscle tissues. This gene has been reported previously in obesity networks and has even been validated by RT-PCR [59,60], however this is the first time that it has been reported in both in VAT and SMT in boys with obesity. This gene and its connected hubs within the green-yellow cluster are more examples of potential polygenetic molecular mechanisms that might underlie the well-known muscle-adipose tissue cross-talk in obesity and metabolic dysfunction.

One of the main restrictions of our study is the low number of participants considered and the need for a validation population, which may have resulted in co-expression networks with spurious correlations. Because of this, in this work, we have tried to minimize these effects by employing strict selection criteria based on the biological consistency of the correlation of clusters with cardiometabolic traits. Another restriction is that the obesity networks referred only to boys, a larger sample size being necessary to extend our findings toward both sexes. However, any children in the population showed signs of puberty entrance, along with there was a high homogeneity in terms of age ranges and sexual maturation status among the recruited children. Therefore, we reduced inter-individual variability to the furthest extent. One of the greatest strengths of this study is the application of a co-expression unsupervised clustering method that looks for co-expression patterns from collected sample biopsies from VAT and SMT, that are rarely accessible in the context of childhood obesity. However, given the limitations of this study, our results should be viewed as an exploratory approach and further confirmed with additional populations.

As future lines of research, the possibility of using other ML techniques with a larger data set, such as classification models using hub genes of selected modules as obesity predictors, could provide essential information on the role of these genes in the pathology. Some advanced pre-processing methods for feature selection; such as wrapper recursive feature elimination [1] and relative weighted consistency [2, 3], could be proposed as feature selection methods in further analyses. Specially, the application of feature selection methods based on the generation of ML models, such as elastic-net, would be of great relevance for researchers with small sample sizes like ours, since they are designed to deal with overfitting and reduce false positive rates [4, 5]. In our case, we selected a traditional but equally valid method based on DE genes because we wanted to focus on the biological relevance and comprehensibility of the clustering algorithm with micro-array [6, 7, 8].

5. Conclusions

Our work identified both independent and inter-tissue gene co-expression patterns correlated with obesity and cardiovascular and altered metabolism risk in the VAT and SMT of prepubertal children. In particular, our inter-tissue WGCNA approach III in VAT and SMT identified several interesting sets of genes co-expressed in both tissues for which prior evidence has been reported in the literature referring to obesity and altered metabolic pathways, along with novel molecular targets previously unknown. To the best of our knowledge, this study is the first WGCNA study applied to childhood obesity, that further evaluates the interwoven transcriptomic relationships between VAT and SMT in the context of the pathology. This work generates interesting hypotheses on the transcriptomic alterations underlying metabolic health alterations in obesity in the pediatric population and highlights new potential molecular targets such as *PIK3R2, PPP3C* and *PTPN5*.

Ethics approval

Written consent from children's legal guardians was acquired and all children agreed to participate. The current protocol (07/19/06) was authorized by the Ethics Committee of the Reina Sofia Hospital, in accordance with the recommendations of the European Union's Good Clinical Practice (Document 111/3976/88 July 1990) and following the Revised Declaration of Helsinki. It was also approved by current Spanish legislation regulating clinical studies with human subjects (RD 223/04 on clinical trials).

Funding

This work was supported by the ERDF/Health Institute Carlos III (grant numbers PI20/00711 and PI20/00563); as well as by the ERDF/Regional Government of Andalusia/Ministry of Economic Transformation, Industry, Knowledge and Universities (grant numbers P18-RT-2248 and B-CTS-536-UGR20).

Declaration of competing interest

The authors declare the following financial interests/personal relationships which may be considered as potential competing interests: C.M. Aguilera reports financial support was provided by ERDF, Health Institute Carlos III, Spanish Ministry of Science. J. Alcala-Fdez reports financial support was provided by ERDF, Regional Government of Andalusia, Ministry of Economic Transformation, Industry, Knowledge and Universities.

Data availability statement

Datasets that reinforce our conclusions have been made open to the public in the Gene Expression Omnibus (GEO) database with the accession codes GSE9624 and GSE139400; corresponding to VAT and SMT, respectively. Software and codes employed for the data analyses have been published in GitHub (i.e., https://github.com/COBLabUGR/WGCNAInterTis sueObesity).

Appendix A. Supplementary data

Supplementary data can be found in the web page that we have developed for this study (i.e., https://sci2s.ugr.es/WGCNAInterTissue Obesitys).

Appendix B. Abbreviations

- *Apo-A*: Apolipoprotein A1
- *Apo-B*: Apolipoprotein B
- *BMI*: Body mass index
- *CVD*: Cardiometabolic risk disease
- *DBP*: Diastolic blood pressure
- *DE*: Differentially expressed
- *GEO*: Gene expression omnibus
- *GO*: Gene ontology
- *HDL-c*: High-density lipoprotein cholesterol
- *HOMA*: Homeostatic assessment model
- *KEGG*: Kyoto encyclopedia of genes and genomes
- *LDL-c*: Low-density lipoprotein cholesterol
- *ML*: Machine learning
- *MM*: Cluster membership
- *NAFLD*: Non-alcoholic fatty liver disease
- *QUICKI*: Insulin sensitivity check index
- *r*: Scale-free topology model fit indexes
- R^2: Correlation coefficient
- *SBP*: Systolic blood pressure
- *SMT*: Skeletal muscle tissue
- *SREBP*, sterol regulatory element binding protein.
- *T2D*: Type 2 diabetes
- *TOM*: Topological overlap measure
- *VAT*: Visceral adipose tissue
- *WGCNA*: Weighted gene co-expression network analysis

References

[1] N. Koyuncuoglu Gungor, Overweight and obesity in children and adolescents, J. Clin. Res. Pediatr. Endocrinol. 6 (2014) 129–143, http://dx.doi.org/10.4274/jcrpe.1471.
[2] R.M. De Bruyne, E. Fitzpatrick, A. Dhawan, Fatty liver disease in children: Eat now pay later, Hepatol. Int. 4 (1) (2010) 375–385, http://dx.doi.org/10.1007/s12072-009-9160-z.
[3] B.B. Duncan, M.I. Schmidt, J.S. Pankow, C.M. Ballantyne, D. Couper, A. Vigo, R. Hoogeveen, A.R. Folsom, G. Heiss, Low-grade systemic inflammation and the development of type 2 diabetes: The atherosclerosis risk in communities study, Diabetes 52 (7) (2003) 1799–1805, http://dx.doi.org/10.2337/diabetes.52.7.1799.
[4] P. Libby, P.M. Ridker, A. Maseri, Inflammation and atherosclerosis, Circulation 105 (9) (2002) 1135–1143, http://dx.doi.org/10.1161/hc0902.104353.
[5] G. Maurizi, L. Della Guardia, A. Maurizi, A. Poloni, Adipocytes properties and crosstalk with immune system in obesity-related inflammation, J. Cell. Physiol. 233 (1) (2018) 88–97, http://dx.doi.org/10.1002/jcp.25855.
[6] A. Gil, J. Olza, M. Gil-Campos, C. Gomez-Llorente, C.M. Aguilera, Is adipose tissue metabolically different at different sites? Int. J. Pediatr. Obes. 6 (sup1) (2011) 13–20, http://dx.doi.org/10.3109/17477166.2011.604326.
[7] H. Wu, C.M. Ballantyne, Skeletal muscle inflammation and insulin resistance in obesity, J. Clin. Invest. 127 (1) (2017) 43–54, http://dx.doi.org/10.1172/JCI88880.
[8] K.I. Stanford, L.J. Goodyear, Muscle-adipose tissue cross talk, Cold Spring Harb. Perspect. Med. 8 (8) (2018) a029801, http://dx.doi.org/10.1101/cshperspect.a029801.
[9] O. Sarr, R.J. Strohm, T.L. Macdonald, N. Gaudio, J.K. Reed, J. Foute-Nelong, D.J. Dyck, D.M. Mutch, Subcutaneous and visceral adipose tissue secretions from extremely obese men and women both acutely suppress muscle insulin signaling, Int. J. Mol. Sci. 18 (5) (2017) 959, http://dx.doi.org/10.3390/ijms18050959.
[10] G.R. Hajer, T.W. van Haeften, F.L. Visseren, Adipose tissue dysfunction in obesity, diabetes, and vascular diseases, Eur. Heart J. 29 (24) (2008) 2959–2971, http://dx.doi.org/10.1093/eurheartj/ehn387.
[11] K. Williams, L.R. Ingerslev, J. Bork-Jensen, M. Wohlwend, A.N. Hansen, L. Small, R. Ribel-Madsen, A. Astrup, O. Pedersen, J. Auwerx, C.T. Workman, N. Grarup, T. Hansen, R. Barrès, Skeletal muscle enhancer interactions identify genes controlling whole-body metabolism, Nature Commun. 11 (1) (2020) 2695, http://dx.doi.org/10.1038/s41467-020-16537-6.
[12] L.J. Kogelman, J. Fu, L. Franke, J.W. Greve, M. Hofker, S.S. Rensen, H.N. Kadarmideen, Inter-tissue gene co-expression networks between metabolically healthy and unhealthy obese individuals, PLoS One 11 (12) (2016) e0167519, http://dx.doi.org/10.1371/journal.pone.0167519.
[13] J.N. Weiss, A. Karma, W.R. MacLellan, M. Deng, C.D. Rau, C.M. Rees, J. Wang, N. Wisniewski, E. Eskin, S. Horvath, Z. Qu, Y. Wang, A.J. Lusis, "Good Enough Solutions" and the genetics of complex diseases, Circ. Res. 111 (4) (2012) 493–504, http://dx.doi.org/10.1161/CIRCRESAHA.112.269084.
[14] M.W. Libbrecht, W.S. Noble, Machine learning applications in genetics and genomics, Nature Rev. Genet. 16 (6) (2015) 321–332, http://dx.doi.org/10.1038/nrg3920.
[15] A. Anguita-Ruiz, A. Segura-Delgado, R. Alcalá, C.M. Aguilera, J. Alcalá-Fdez, eXplainable Artificial Intelligence (XAI) for the identification of biologically relevant gene expression patterns in longitudinal human studies, insights from obesity research, PLoS Comput. Biol. 16 (4) (2020) e1007792, http://dx.doi.org/10.1371/journal.pcbi.1007792.
[16] A. Barredo Arrieta, N. Díaz-Rodríguez, J. Del Ser, A. Bennetot, S. Tabik, A. Barbado, S. Garcia, S. Gil-Lopez, D. Molina, R. Benjamins, R. Chatila, F. Herrera, Explainable Artificial Intelligence (XAI): Concepts, taxonomies, opportunities and challenges toward responsible AI, Inf. Fusion 58 (2020) 82–115, http://dx.doi.org/10.1016/j.inffus.2019.12.012.
[17] A. Fernandez, F. Herrera, O. Cordon, M. Jose del Jesus, F. Marcelloni, Evolutionary fuzzy systems for explainable artificial intelligence: Why, when, what for, and where to? IEEE Comput. Intell. Mag. 14 (1) (2019) 69–81, http://dx.doi.org/10.1109/MCI.2018.2881645.
[18] P.C. Phillips, Epistasis - The essential role of gene interactions in the structure and evolution of genetic systems, Nature Rev. Genet. 9 (11) (2008) 855–867, http://dx.doi.org/10.1038/nrg2452.
[19] Y. Hu, M. Li, Q. Lu, H. Weng, J. Wang, S.M. Zekavat, Z. Yu, B. Li, J. Gu, S. Muchnik, Y. Shi, B.W. Kunkle, S. Mukherjee, P. Natarajan, A. Naj, A. Kuzma, Y. Zhao, P.K. Crane, H. Lu, H. Zhao, A statistical framework for cross-tissue transcriptome-wide association analysis, Nature Genet. 51 (3) (2019) 568–576, http://dx.doi.org/10.1038/s41588-019-0345-7.
[20] B. Zhang, S. Horvath, A general framework for weighted gene co-expression network analysis, Stat. Appl. Genet. Mol. Biol. 4 (1) (2005) 17, http://dx.doi.org/10.2202/1544-6115.1128.
[21] P. Langfelder, S. Horvath, WGCNA: an R package for weighted correlation network analysis, BMC Bioinformatics 9 (1) (2008) 559, http://dx.doi.org/10.1186/1471-2105-9-559.
[22] T.J. Cole, Establishing a standard definition for child overweight and obesity worldwide: international survey, BMJ 320 (7244) (2000) 1240, http://dx.doi.org/10.1136/bmj.320.7244.1240.

[23] J.M. Tanner, R.H. Whitehouse, Clinical longitudinal standards for height, weight, height velocity, weight velocity, and stages of puberty, Arch. Dis. Child. 51 (3) (1976) 170–179, http://dx.doi.org/10.1136/adc.51.3.170.
[24] C.M. Aguilera, C. Gomez-Llorente, I. Tofe, M. Gil-Campos, R. Cañete, Á. Gil, Genome-wide expression in visceral adipose tissue from obese prepubertal children, Int. J. Mol. Sci. 16 (4) (2015) 7723–7737, http://dx.doi.org/10.3390/ijms16047723.
[25] B. Sobradillo, A. Aguirre, U. Aresti, A. Bilbao, C. Fernández-Ramos, A. Lizárraga, H. Lorenzo, L. Madariaga, I. Rica, I. Ruiz, Curvas y tablas de crecimiento (estudios longitudinal y transversal), Inst. Investig. sobre crecimiento desarrollo. Fundación Faustino Orbegozo 36 (2004).
[26] B.W. McCrindle, Assessment and management of hypertension in children and adolescents, Nat. Rev. Cardiol. 7 (3) (2010) 155–163, http://dx.doi.org/10.1038/nrcardio.2009.231.
[27] D.R. Matthews, J.P. Hosker, A.S. Rudenski, B.A. Naylor, D.F. Treacher, R.C. Turner, Homeostasis model assessment: insulin resistance and ?-cell function from fasting plasma glucose and insulin concentrations in man, Diabetologia 28 (7) (1985) 412–419, http://dx.doi.org/10.1007/BF00280883.
[28] A. Katz, S.S. Nambi, K. Mather, A.D. Baron, D.A. Follmann, G. Sullivan, M.J. Quon, Quantitative insulin sensitivity check index: A simple, accurate method for assessing insulin sensitivity in humans, J. Clin. Endocrinol. Metab. 85 (7) (2000) 2402–2410, http://dx.doi.org/10.1210/jcem.85.7.6661.
[29] R. Ihaka, R. Gentleman, R: A language for data analysis and graphics, J. Comput. Graph. Statist. 5 (3) (1996) 299–314, http://dx.doi.org/10.2307/1390807.
[30] E. Saccenti, Correlation patterns in experimental data are affected by normalization procedures: Consequences for data analysis and network inference, J. Proteome Res. 16 (2) (2017) 619–634, http://dx.doi.org/10.1021/acs.jproteome.6b00704.
[31] E. Freyhult, M. Landfors, J. Önskog, T.R. Hvidsten, P. Rydén, Challenges in microarray class discovery: A comprehensive examination of normalization, gene selection and clustering, BMC Bioinformatics 11 (2010) 503, http://dx.doi.org/10.1186/1471-2105-11-503.
[32] M. Carlson, org.Hs.eg.db: Genome wide annotation for human, 2020, R package version 3.8.2.
[33] A.W.-C. Liew, N.-F. Law, H. Yan, Missing value imputation for gene expression data: computational techniques to recover missing data from available information, Brief. Bioinform. 12 (5) (2011) 498–513, http://dx.doi.org/10.1093/bib/bbq080.
[34] S. Boluki, S. Zamani Dadaneh, X. Qian, E.R. Dougherty, Optimal clustering with missing values, BMC Bioinformatics 20 (S12) (2019) 321, http://dx.doi.org/10.1186/s12859-019-2832-3.
[35] M.C. de Souto, P.A. Jaskowiak, I.G. Costa, Impact of missing data imputation methods on gene expression clustering and classification, BMC Bioinformatics 16 (1) (2015) 64, http://dx.doi.org/10.1186/s12859-015-0494-3.
[36] J.G. Dy, C.E. Brodley, Feature selection for unsupervised learning, J. Mach. Learn. Res. 5 (2004) 845–889, http://dx.doi.org/10.5555/1005332.1016787.
[37] C.G. Saris, S. Horvath, P.W. van Vught, M.A. van Es, H.M. Blauw, T.F. Fuller, P. Langfelder, J. DeYoung, J.H. Wokke, J.H. Veldink, L.H. van den Berg, R.A. Ophoff, Weighted gene co-expression network analysis of the peripheral blood from Amyotrophic Lateral Sclerosis patients, BMC Genomics 10 (1) (2009) 405, http://dx.doi.org/10.1186/1471-2164-10-405.
[38] P. Langfelder, R. Luo, M.C. Oldham, S. Horvath, Is my network module preserved and reproducible? PLoS Comput. Biol. 7 (1) (2011) e1001057, http://dx.doi.org/10.1371/journal.pcbi.1001057.
[39] W. Zhao, P. Langfelder, T. Fuller, J. Dong, A. Li, S. Hovarth, Weighted gene coexpression network analysis: State of the art, J. Biopharm. Statist. 20 (2) (2010) 281–300, http://dx.doi.org/10.1080/10543400903572753.
[40] P. Langfelder, S. Horvath, Fast R functions for robust correlations and hierarchical clustering, J. Stat. Softw. 46 (11) (2012) i11, http://dx.doi.org/10.18637/jss.v046.i11.
[41] B. Cox, M. Tsamou, K. Vrijens, K.Y. Neven, E. Winckelmans, T.M. de Kok, M. Plusquin, T.S. Nawrot, A co-expression analysis of the placental transcriptome in association with maternal pre-pregnancy BMI and newborn birth weight, Front. Genet. 10 (2019) 354, http://dx.doi.org/10.3389/fgene.2019.00354.
[42] M. Ashburner, C.A. Ball, J.A. Blake, D. Botstein, H. Butler, J.M. Cherry, A.P. Davis, K. Dolinski, S.S. Dwight, J.T. Eppig, M.A. Harris, D.P. Hill, L. Issel-Tarver, A. Kasarskis, S. Lewis, J.C. Matese, J.E. Richardson, M. Ringwald, G.M. Rubin, G. Sherlock, Gene ontology: Tool for the unification of biology. The gene ontology consortium, Nature Genet. 25 (1) (2000) 25–29, http://dx.doi.org/10.1038/75556.
[43] M. Kanehisa, S. Goto, Y. Sato, M. Furumichi, M. Tanabe, KEGG for integration and interpretation of large-scale molecular data sets, Nucleic Acids Res. 40 (D1) (2012) D109–D114, http://dx.doi.org/10.1093/nar/gkr988.
[44] M. Gaggini, M. Morelli, E. Buzzigoli, R.A. DeFronzo, E. Bugianesi, A. Gastaldelli, Non-alcoholic fatty liver disease (NAFLD) and its connection with insulin resistance, dyslipidemia, atherosclerosis and coronary heart disease, Nutrients 5 (5) (2013) 1544–1560, http://dx.doi.org/10.3390/nu5051544.
[45] J.A. Paniagua, J.M. Escandell-Morales, D. Gil-Contreras, F.J. Berral de la Rosa, M. Romero-Jimenez, A. Gómez-Urbano, A. Sanchez-Lopez, E. Bellido, A. Poyato, B. Calatayud, A.J. Vidal-Puig, Central obesity and altered peripheral adipose tissue gene expression characterize the NAFLD patient with insulin resistance: Role of nutrition and insulin challenge, Nutrition 30 (2) (2014) 177–185, http://dx.doi.org/10.1016/j.nut.2013.07.017.
[46] M. Martínez-Uña, Y. López-Mancheño, C. Diéguez, M.A. Fernández-Rojo, M.G. Novelle, Unraveling the role of leptin in liver function and its relationship with liver diseases, Int. J. Mol. Sci. 21 (24) (2020) 1–33, http://dx.doi.org/10.3390/ijms21249368.
[47] A. Ardestani, B. Lupse, K. Maedler, Hippo signaling: Key emerging pathway in cellular and whole-body metabolism, Trends Endocrinol. Metabol. 29 (7) (2018) 492–509, http://dx.doi.org/10.1016/j.tem.2018.04.006.
[48] K.I. Watt, C.A. Goodman, T.A. Hornberger, P. Gregorevic, The hippo signaling pathway in the regulation of skeletal muscle mass and function, Exerc. Sport Sci. Rev. 46 (2) (2018) 92–96, http://dx.doi.org/10.1249/JES.0000000000000142.
[49] F. Riuzzi, G. Sorci, R. Sagheddu, S. Chiappalupi, L. Salvadori, R. Donato, RAGE in the pathophysiology of skeletal muscle, J. Cachexia Sarcopenia Muscle 9 (7) (2018) 1213–1234, http://dx.doi.org/10.1002/jcsm.12350.
[50] I. Sinha, D. Sakthivel, D.E. Varon, Systemic regulators of skeletal muscle regeneration in obesity, Front. Endocrinol. 8 (2017) http://dx.doi.org/10.3389/fendo.2017.00029.
[51] J. Farup, L. Madaro, P.L. Puri, U.R. Mikkelsen, Interactions between muscle stem cells, mesenchymal-derived cells and immune cells in muscle homeostasis, regeneration and disease, Cell Death Dis. 6 (7) (2015) http://dx.doi.org/10.1038/cddis.2015.198.
[52] K.E. Kypreos, E.A. Karavia, C. Constantinou, A. Hatziri, C. Kalogeropoulou, E. Xepapadaki, E. Zvintzou, Apolipoprotein E in diet-induced obesity: a paradigm shift from conventional perception, J. Biomed. Res. 32 (3) (2017) 183–190, http://dx.doi.org/10.7555/JBR.32.20180007.
[53] V. Vincent, H. Thakkar, S. Aggarwal, A. Mridha, L. Ramakrishnan, A. Singh, ATP-binding cassette transporter A1 (ABCA 1) expression in adipose tissue and its modulation with insulin resistance in obesity [corrigendum], Diabetes Metab. Syndr. Obes. 12 (2019) 2633.
[54] H.F. Kramer, L.J. Goodyear, Exercise, MAPK, and NF-KB signaling in skeletal muscle, J. Appl. Physiol. 103 (1) (2007) 388–395, http://dx.doi.org/10.1152/japplphysiol.00085.2007.
[55] N. Adi, C. Perriotte-Olson, V.C. Desouza, R. Ramalingam, V. Saraswathi, Hematopoietic cyclooxygenase-2 deficiency increases adipose tissue inflammation and adiposity in obesity, Obesity 23 (10) (2015) 2037–2045, http://dx.doi.org/10.1002/oby.21184.
[56] Y.J. Liu, Y.F. Guo, L.S. Zhang, Y.F. Pei, N. Yu, P. Yu, C.J. Papasian, H.W. Deng, Biological pathway-based genome-wide association analysis identified the vasoactive intestinal peptide (VIP) pathway important for obesity, Obesity (Silver Spring) 18 (12) (2010) 2339–2346, http://dx.doi.org/10.1038/oby.2010.83.
[57] H. Yamakage, Y. Konishi, K. Muranaka, K. Hotta, Y. Miyamoto, H. Morisaki, T. Morisaki, N. Satoh-Asahara, Association of protein tyrosine phosphatase 1B gene polymorphism with the effects of weight reduction therapy on bodyweight and glycolipid profiles in obese patients, J. Diabetes Investig. 12 (8) (2021) 1462–1470, http://dx.doi.org/10.1111/jdi.13492.
[58] C. Cheyssac, C. Lecoeur, A. Dechaume, A. Bibi, G. Charpentier, B. Balkau, M. Marre, P. Froguel, F. Gibson, M. Vaxillaire, Analysis of common PTPN1gene variants in type 2 diabetes, obesity and associated phenotypes in the french population, BMC Med. Genet. 7 (1) (2006) http://dx.doi.org/10.1186/1471-2350-7-44.
[59] G. Prashanth, B. Vastrad, A. Tengli, C. Vastrad, I. Kottursheti, Investigation of candidate genes and mechanisms underlying obesity associated type 2 diabetes mellitus using bioinformatics analysis and screening of small drug molecules, BMC Endocr. Disord. 21 (1) (2021) http://dx.doi.org/10.1186/s12902-021-00718-5.
[60] D. Masih, J.K. Tripathi, G. Rakhra, A. Vats, S.K. Verma, P.K. Jha, M. Sharma, M.Z. Ashraf, S.N. Singh, Deciphering biochemical and molecular signatures associated with obesity in context of metabolic health, Genes 12 (2) (2021) 290, http://dx.doi.org/10.3390/genes12020290.